

OSU-A9, a potent indole-3-carbinol derivative, suppresses breast tumor growth by targeting the Akt–NF- κ B pathway and stress response signaling

Jing-Ru Weng, Chen-Hsun Tsai¹, Hany A.Omar¹, Aaron M.Sargeant^{1,2}, Dasheng Wang¹, Samuel K.Kulp¹, Charles L.Shapiro³ and Ching-Shih Chen^{1,*}

Department of Biological Science and Technology, China Medical University, Taichung 40402, Taiwan and ¹Division of Medicinal Chemistry, College of Pharmacy, ²Department of Veterinary Biosciences, College of Veterinary Medicine and ³Division of Hematology and Oncology, Department of Internal Medicine, The Ohio State University, Columbus, OH 43210, USA

*To whom correspondence should be addressed. Division of Medicinal Chemistry, College of Pharmacy, Parks Hall, The Ohio State University, 500 West 12th Avenue, Columbus, OH 43210, USA. Tel: +1 614 688 4008; Fax: +1 614 688 8556; Email: chen.844@osu.edu

The molecular heterogeneity of human tumors challenges the development of effective preventive and therapeutic strategies. To overcome this issue, a rational approach is the concomitant targeting of clinically relevant cellular abnormalities with combination therapy or a potent multi-targeted agent. OSU-A9 is a novel indole-3-carbinol derivative that retains the parent compound's ability to perturb multiple components of oncogenic signaling, but provides marked advantages in chemical stability and antitumor potency. Here, we show that OSU-A9 exhibits two orders of magnitude greater potency than indole-3-carbinol in inducing apoptosis in various breast cancer cell lines with distinct genetic abnormalities, including MCF-7, MDA-MB-231 and SKBR3, with the half maximal inhibitory concentration in the range of 1.2–1.8 μ M vis-à-vis 200 μ M for indole-3-carbinol. This differential potency was paralleled by OSU-A9's superior activity against multiple components of the Akt–nuclear factor-kappa B (NF- κ B) and stress response signaling pathways. Notable among these were the increased estrogen receptor (ER)- β /ER α expression ratio, reduced expression of HER2 and CXCR4 and the upregulation of aryl hydrocarbon receptor expression and its downstream target NF-E2 p45-regulated factor (Nrf2). Non-malignant MCF-10A cells were resistant to OSU-A9's antiproliferative effects. Daily oral administration of OSU-A9 at 25 and 50 mg/kg for 49 days significantly inhibited MCF-7 tumor growth by 59 and 70%, respectively, without overt signs of toxicity or evidence of induced hepatic biotransformation enzymes. In summary, OSU-A9 is a potent, orally bioavailable inhibitor of the Akt–NF- κ B signaling network, targeting multiple aspects of breast tumor pathogenesis and progression. Thus, its translational potential for the treatment or prevention of breast cancer warrants further investigation.

Introduction

During the course of carcinogenesis and tumor progression, cancer cells overcome genomic and cellular abnormalities by constitutively upregulating a diversity of signaling pathways governing cell proliferation, survival, hormonal homeostasis, invasion, metastasis and drug resistance. In light of this heterogeneity, it is desirable to concomitantly target multiple clinically relevant cellular defects by using a combination treatment or a multi-targeted antitumor agent to opti-

Abbreviations: AhR, aryl hydrocarbon receptor; DMSO, dimethyl sulfoxide; ER, estrogen receptor; FBS, fetal bovine serum; GSK, glycogen synthase kinase; IKK, I κ B kinase; MTT, 3-(4,5-dimethylthiazol-2-yl)-2,5-diphenyl-2H-tetrazolium bromide; NF- κ B, nuclear factor-kappa B; Nrf2, NF-E2 p45-regulated factor; PBS, phosphate-buffered saline; PARP, poly(adenine dinucleotide phosphate-ribose) polymerase; TBST, Tris-buffered saline containing 0.05% Tween 20.

mize therapeutic outcomes (1). This underlying principle constitutes a basis for the clinical trial of indole-3-carbinol in breast cancer prevention (2,3). Mounting evidence indicates that the antitumor effects of indole-3-carbinol are attributed to its ability to interfere with multiple facets of oncogenic signaling pathways (reviewed in refs 4–8). Moreover, indole-3-carbinol proved to be an effective chemopreventive agent against estrogen-responsive cancers, in part, because of its activity as a negative regulator of estrogen action through inhibition of estrogen receptor (ER)- α signaling (9,10) and modulation of cytochrome P450-mediated estrogen metabolism (11). However, several factors compromise the *in vivo* efficacy of indole-3-carbinol, including low *in vitro* antitumor potency, limited bioavailability and complicated pharmacokinetic behaviors due to intrinsic metabolic instability (8). Consequently, the structural optimization of indole-3-carbinol or its metabolite 3,3'-diindolymethane to develop novel indole derivatives with improved potency and metabolic stability has been the focus of many recent investigations. This drug development effort has led to several potent antitumor agents with distinct pharmacological activities, including SRI3668 (an Akt inhibitor) (12), 1-(*p*-substituted phenyl)-3,3'-diindolymethane (nuclear receptor agonists) (13,14), a tetrameric derivative (a cyclin-dependent kinase 6 inhibitor) (15) and OSU-A9 (a multi-targeted agent) (16). From a translational perspective, OSU-A9 provides considerable therapeutic advantage over indole-3-carbinol with respect to chemical stability and antitumor potency (16). In this study, we show that OSU-A9 exhibits *in vitro* potency that is two orders of magnitude higher than that of indole-3-carbinol in suppressing the proliferation of breast tumor cells. Previously, we demonstrated that OSU-A9 disrupted a broad spectrum of signaling pathways involved in the regulation of cell cycle progression and cell survival (16). In this study, mechanistic evidence further attributes the growth-inhibitory effect of OSU-A9 to its ability to modulate Akt/nuclear factor-kappa B (NF- κ B)- and stress-induced signaling networks, paralleling that of indole-3-carbinol. Equally important, oral OSU-A9 inhibited MCF-7 xenograft tumor growth *in vivo* without incurring overt signs of toxicity or significant loss of body weight compared with vehicle-treated controls. These results indicate the translational potential of OSU-A9 as a component of chemotherapeutic and/or chemopreventive strategies for breast cancer.

Materials and methods

Reagents, antibodies and plasmids

1H-indole-3-carbinol and OSU-A9 {[1-(4-chloro-3-nitrobenzenesulfonyl)-1H-indol-3-yl]-methanol} were synthesized as described previously (16), of which the identity and purity ($\geq 99\%$) were verified by proton nuclear magnetic resonance, high-resolution mass spectrometry and elemental analysis. For *in vitro* experiments, these agents at various concentrations were dissolved in dimethyl sulfoxide (DMSO), diluted in culture medium and added to cells at a final DMSO concentration of 0.1%. For *in vivo* studies, OSU-A9 was prepared as a suspension in vehicle (0.5% methylcellulose and 0.1% Tween 80 in sterile water) for oral administration to tumor-bearing immunocompromised mice. Rabbit polyclonal antibodies against various biomarkers were obtained from the following sources: p-⁴⁷³Ser Akt, I κ B kinase (IKK)- α , p-¹⁰⁸Ser IKK α , glycogen synthase kinase (GSK)-3 β , p-⁹Ser-GSK3 β , p-¹⁸³Thr/¹⁸⁵Tyr-JNK, JNK, p-¹⁸⁰Thr/¹⁸²Tyr-p38, p38, cyclin D1 and RelA, Cell Signaling Technologies (Beverly, MA); Akt, p27, p21, Bax, Bcl-2, Bcl-xL, Mcl-1, CXCR4, Her2, GADD153, BRCA1, BRCA2, ER α , aryl hydrocarbon receptor (AhR) and NF-E2 p45-regulated factor (Nrf2), Santa Cruz Biotechnology (Santa Cruz, CA); ER β , Abcam (Cambridge, MA); survivin, R&D Systems (Minneapolis, MN); β -actin, Sigma–Aldrich (St Louis, MO). Mouse monoclonal anti-poly(adenine dinucleotide phosphate-ribose) polymerase (PARP) antibody was purchased from Pharmingen (San Diego, CA). The enhanced chemiluminescence system for detection of immunoblotted proteins was from GE Healthcare Bioscience (Piscataway, NJ). Other chemicals and biochemistry reagents were obtained

from Sigma–Aldrich unless otherwise mentioned. The pNF- κ B-Luc reporter plasmid was kindly provided by Dr Cheng-Wen Lin, China Medical University, Taichung, Taiwan, and the Renilla Luciferase Control Reporter Vector (pRL-CMV) was purchased from Promega (Madison, WI).

Cell culture

MCF-7 (ER α +/ β +, Her2– and p53+), SKBR3 (ER α –/ β –, Her2+ and p53–) and MDA-MB-231 (ER α –/ β +, Her2– and p53–) human breast cancer cells were purchased from American Type Tissue Collection (Manassas, VA) and cultured in Dulbecco's modified Eagle's medium/F12 medium (Gibco, Grand Island, NY) supplemented with 10% fetal bovine serum (FBS; Gibco). MCF-10A non-malignant breast epithelial cells were kindly provided by Dr Robert Brueggemeier (The Ohio State University) and maintained in the same medium supplemented with 5% FBS, 100 U of penicillin, 100 g/ml streptomycin, 20 ng/ml epidermal growth factor, 10 ng/ml insulin, 100 ng/ml cholera toxin and 500 ng/ml hydrocortisone. All cell types were cultured at 37°C in a humidified incubator containing 5% CO₂.

Cell viability analysis

The effect of test agents on cell viability was assessed by using the 3-(4,5-dimethylthiazol-2-yl)-2,5-diphenyl-2H-tetrazolium bromide (MTT) assay in 6–12 replicates. Cancer cells and MCF-10A cells were grown in 5% FBS-supplemented Dulbecco's modified Eagle's medium/F12 medium or 5% FBS-supplemented Dulbecco's modified Eagle's medium/F12 medium containing 20 ng/ml epidermal growth factor, 100 ng/ml cholera toxin and 500 ng/ml hydrocortisone, respectively, in 96-well, flat-bottomed plates for 24 h and then exposed to various concentrations of test agents in the respective medium for the indicated time intervals. Controls received DMSO vehicle at a concentration equal to that in drug-treated cells. At the end of treatments, the medium was replaced by 200 μ l of 0.5 mg/ml of MTT in the same medium, and cells were incubated in the CO₂ incubator at 37°C for 2 h. Supernatants were removed from the wells, and the reduced MTT dye was solubilized in 200 μ l per well of DMSO. Absorbance at 570 nm was determined on a microplate reader.

Immunoblotting

Biomarkers of apoptosis and signaling pathway components associated with cell survival and growth arrest were assessed by western immunoblotting as follows. Treated cells were washed with phosphate-buffered saline (PBS), resuspended in sodium dodecyl sulfate sample buffer, sonicated for 5 s, and then boiled for 5 min. After brief centrifugation, equivalent amounts of proteins from the soluble fractions of cell lysates were resolved in 10% sodium dodecyl sulfate–polyacrylamide gels on a Minigel apparatus, and transferred to a nitrocellulose membrane using a semidry transfer cell. The transblotted membrane was washed three times with Tris-buffered saline containing 0.05% Tween 20 (TBST). After blocking with TBST containing 5% non-fat milk for 60 min, the membrane was incubated with an appropriate primary antibody at 1:500 dilution (with the exception of anti- β -actin antibody, 1:2000) in TBST–5% low fat milk at 4°C for 12 h and was then washed three times with TBST. The membrane was probed with goat anti-rabbit or anti-mouse IgG-horseradish peroxidase conjugates (1:2500) for 90 min at room temperature and washed three times with TBST. The immunoblots were visualized by enhanced chemiluminescence.

Cell cycle analysis

Cell cycle distribution was determined by flow cytometric analysis of propidium iodide-stained cellular DNA. Briefly, MCF-7 cells were incubated with the indicated concentrations of OSU-A9 for 24 h, harvested, washed with PBS and then fixed overnight in 40% ethanol (in PBS, vol/vol). Following rehydration in PBS, cells were exposed to 5 μ g/ml of propidium iodide (in PBS) in the presence of ribonuclease A (50 U/ml) at room temperature for 30 min to label DNA. The percentage of cells in each of the phases of the cell cycle was determined using a fluorescence-activated cell sorter (FACSCalibur, Becton Dickinson Immunocytometry Systems) equipped with ModFiLT V3.0 software.

NF- κ B-dependent reporter gene expression assay

Between 1×10^6 and 3×10^6 MCF-7 cells were transiently cotransfected with 2 μ g of the pNF- κ B-Luc reporter plasmid and 0.5 μ g of the Renilla Luciferase Control Reporter Vector (pRL-CMV) using the Amaxa® Nucleofector system (Gaithersburg, MD). Transfected cells were seeded into 12-well plates and cultured for 24 h, after which cells were treated in triplicate with different concentrations of OSU-A9 or vehicle in the presence or absence of 0.1 nM tumor necrosis factor- α (PeproTech, Rocky Hill, NJ) for 6 h. The luciferase activities present in the cell lysates were determined using the Dual-Luciferase® Reporter Assay System (Promega) and normalized to the constitutive Renilla luciferase activity.

In vivo studies

Female ovariectomized NCr athymic nude mice (5–7 weeks of age) were obtained from the National Cancer Institute (Frederick, MD). Mice were group-housed under conditions of constant photoperiod (12 h light: 12 h dark) with *ad libitum* access to sterilized food and water. All experimental procedures utilizing these mice were performed in accordance with protocols approved by the Institutional Laboratory Animal Care and Use Committee of The Ohio State University. After acclimatization, a 17- β estradiol-containing continuous-release pellet (0.72 mg per pellet, 60 day release, Innovative Research of America, Sarasota, FL) was implanted subcutaneously in the interscapular region of each mouse using a 10 ga trocar. Two days later, each mouse was inoculated subcutaneously in the right flank with 2×10^6 MCF-7 cells in a total volume of 0.1 ml of Matrigel (BD Biosciences, Bedford, MA) under isoflurane anesthesia. As tumors became established (mean starting tumor volume, 145 ± 14 mm³), mice were randomized to three groups ($n = 7$) that received the following treatments: (i) OSU-A9 at 25 mg/kg body wt once a day; (ii) OSU-A9 at 50 mg/kg once a day and (iii) methylcellulose/Tween 80 vehicle. Mice received treatments by oral gavage (10 μ l/g body wt) for the duration of the study. Tumors were measured weekly using calipers and their volumes calculated using a standard formula: width² \times length \times 0.52. Body weights were measured weekly. The percentages of reduction in tumor growth were calculated using the formula: $[1 - (T_f - T_i)/(C_f - C_i)] \times 100$, where T_f and T_i are the final and initial mean tumor volumes, respectively, of the group receiving a specified treatment, and C_f and C_i are the final and initial mean tumor volumes, respectively, of the control group. At terminal killing, a complete necropsy was performed on all mice and MCF-7 tumors were harvested. A portion of each tumor was snap-frozen in liquid nitrogen and stored at –80°C until needed for western blot analysis of relevant biomarkers, and the remainder was fixed in 10% formalin. Liver samples were fixed overnight in 10% formalin then transferred to 70% ethanol. Four μ m thick, paraffin-embedded liver tissue sections were stained with hematoxylin and eosin and toluidine blue by standard procedures. Blood from each mouse was submitted to The Ohio State University Veterinary Clinical Laboratory Services for evaluation of serum chemistry and hematological parameters.

Statistical analysis

Each *in vitro* experiment was performed at least two times. The *in vivo* study was performed once. Differences in relative NF- κ B activation *in vitro* and among group means of tumor volume *in vivo* were analyzed for statistical significance using one-way analysis of variance followed by the Neuman–Keuls test for multiple comparisons. Differences were considered significant at $P < 0.05$. Statistical analyses were performed using SPSS for Windows (SPSS, Chicago, IL).

Results

OSU-A9 induces apoptotic death in breast cancer cells with high potency irrespective of genetic abnormalities

The antiproliferative activity of OSU-A9 vis-à-vis indole-3-carbinol was appraised in three human breast cancer cell lines, MCF-7 (ER α +/ β +, Her2– and p53+), SKBR3 (ER α –/ β –, Her2+ and p53–) and MDA-MB-231 (ER α –/ β +, Her2– and p53–), relative to MCF10A non-malignant breast epithelial cells by MTT assay (Figure 1A). OSU-A9 exhibited high potency in suppressing the viability of these breast cancer cells irrespective of differences in genetic abnormalities. The half maximal inhibitory concentration values in MCF-7, SKBR3 and MDA-MB-231 cells were 1.2, 1.6 and 1.8 μ M, respectively, whereas in MCF10A cells it was 7 μ M. In contrast, indole-3-carbinol required a concentration of at least 200 μ M to exhibit an appreciable inhibitory effect on the viability in any of these three cancer cell lines. The antiproliferative effect of OSU-A9 was, at least in part, attributed to its ability to induce apoptosis. Western blot analysis of drug-treated MDA-MB-231 cells showed a dose-dependent effect of both agents on caspase-3 activation and PARP cleavage (Figure 1B), paralleling their respective potencies in suppressing cell viability. In addition, flow cytometric analysis demonstrated a dose-dependent increase in the relative size of the sub-G₁ population of MCF-7 cells, indicative of apoptotic death, after a 48 h exposure to OSU-A9 (Figure 1C).

To shed light onto the mechanism by which OSU-A9 induced apoptosis in breast cancer cells, we investigated the effects of OSU-A9 vis-à-vis indole-3-carbinol on the phosphorylation and/or expression status of a broad spectrum of signaling proteins pertinent to the malignant and invasive phenotypes of breast cancer cells. As

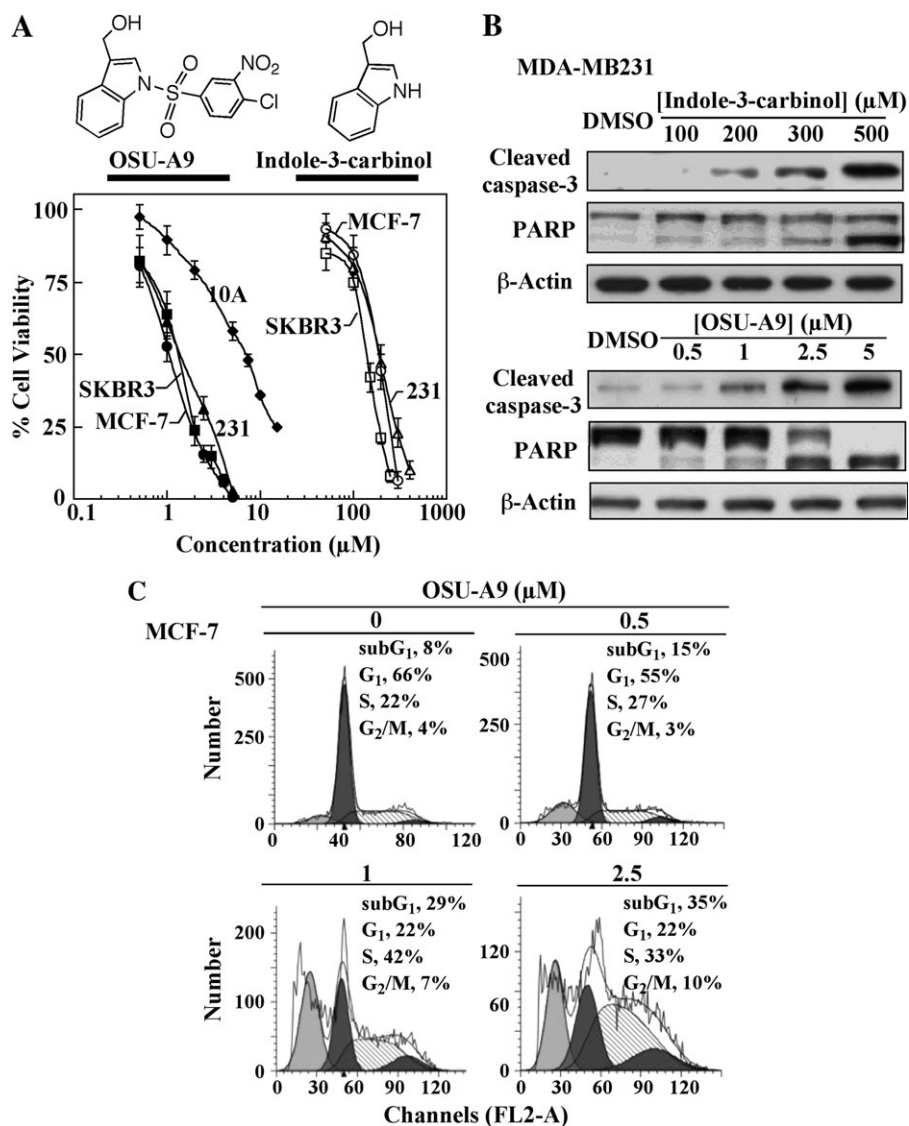


Fig. 1. *In vitro* potencies of OSU-A9 and indole-3-carbinol in inducing apoptotic death in breast cancer cells. (A) Effect of OSU-A9 on the cell viability of MCF-7 (filled circles), SKBR3 (filled squares) and MDA-MB-231 (231; filled triangles) breast cancer cells and MCF-10A non-malignant breast epithelial cells (10A; filled diamonds) versus that of indole-3-carbinol in MCF-7 (open circles), SKBR3 (open squares) and MDA-MB-231 cells (231; open triangles). Cells were treated with OSU-A9 or indole-3-carbinol at the indicated concentrations in 5% FBS-supplemented Dulbecco's modified Eagle's medium/F-12 medium in 96-well plates for 48 h, and cell viability was assessed by MTT assays. Points, mean; bars, standard deviation ($n = 6$). (B) Dose-dependent effect of indole-3-carbinol and OSU-A9 on caspase-3 activation and PARP cleavage in MDA-MB-231 cells after 48 h exposure in 5% FBS-supplemented Dulbecco's modified Eagle's medium/F-12 medium. (C) Flow cytometric analysis of apoptosis in MCF-7 cells after treatment with DMSO vehicle or the indicated concentrations of OSU-A9 for 48 h. The drug-treated cells were fixed and stained with propidium iodide. The extent of apoptosis was assessed by the quantification of sub-2N (sub-G₁) DNA by flow cytometry. The histograms are representative of two independent experiments.

shown in Figures 2 and 3, we obtained evidence that OSU-A9 and indole-3-carbinol exhibited virtually identical pharmacological profiles, albeit with a 100-fold difference in potency, in modulating the functional states of these signaling targets, which could be classified into two categories: the Akt-NF- κ B axis and stress-induced signaling.

The Akt-NF- κ B axis

Data from this and other laboratories suggest that the inactivation of Akt and NF- κ B represents a key event in indole-3-carbinol-mediated antitumor effects (16-18). Similar to indole-3-carbinol, OSU-A9 blocked Akt signaling in MCF-7 cells, as manifested by the concomitant dephosphorylation of Akt and two downstream kinase substrates, GSK3 β and IKK α , in a dose-dependent manner (Figure 2A). Moreover, the dephosphorylating activation of GSK3 β might account for

the reduced expression level of cyclin D1. In addition, two other important cell cycle regulatory proteins, p21 and p27, showed dose-dependent increases in expression in response to either agent, which is in line with earlier reports indicating a mechanistic link between drug-induced Akt inactivation and increased expression of these two cyclin-dependent kinase inhibitors (19,20).

Evidence for the inhibition of NF- κ B signaling by OSU-A9 and indole-3-carbinol points to two distinct mechanisms. First, both agents caused the dose-dependent accumulation of the NF- κ B inhibitor I κ B in MCF-7 cells (Figure 2A), presumably resulting from the observed drug-induced inactivation of IKK α and consequent decrease in I κ B degradation. Second, these agents exhibited a unique ability to suppress the expression of the RelA/p65 subunit of NF- κ B (Figure 2A). Through this concerted mechanism, OSU-A9 dose dependently blocked tumor necrosis factor- α -induced NF- κ B-dependent

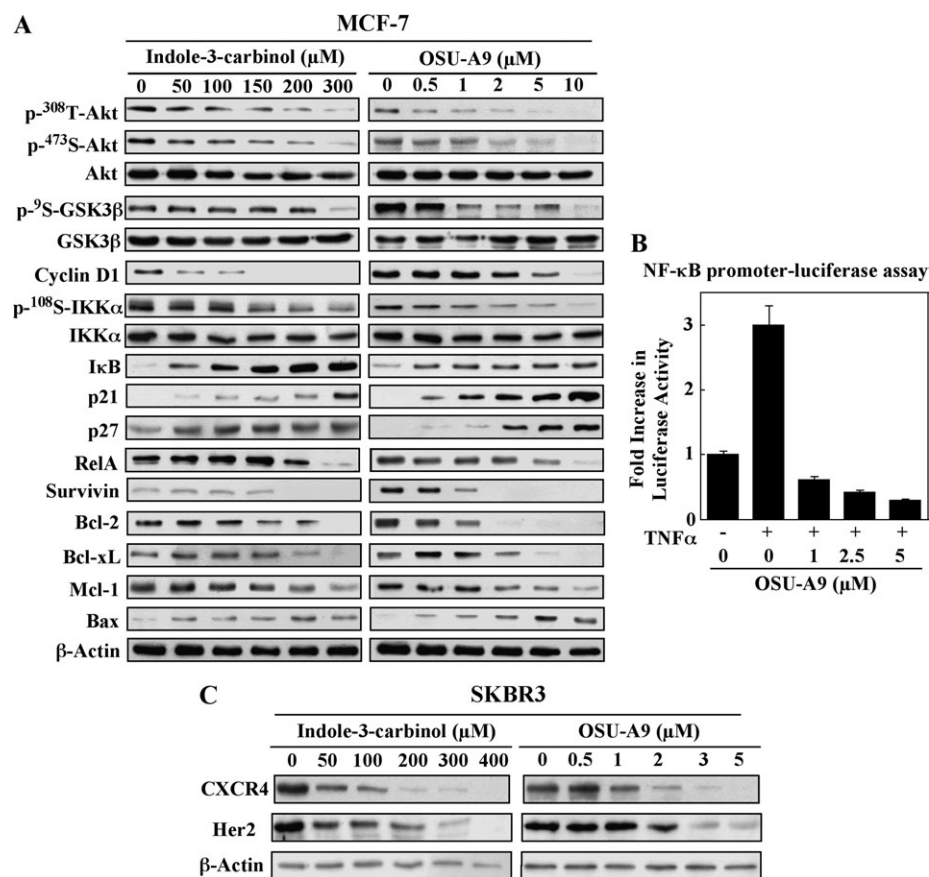


Fig. 2. Inhibition of the Akt–NF- κ B signaling axis by OSU-A9 and indole-3-carbinol. (A) Dose-dependent effects of OSU-A9 versus indole-3-carbinol on the phosphorylation of Akt, GSK3 β and IKK α and the expression levels of cyclin D1, I κ B, p21, p27, RelA, survivin, Bcl-2, Bcl-xL, Mcl-1 and Bax in MCF-7 cells after 48 h exposure in 5% FBS-containing Dulbecco's modified Eagle's medium/F-12 medium. (B) Dose-dependent effect of OSU-A9 on tumor necrosis factor (TNF)- α -activated NF- κ B-mediated transcriptional activity. MCF-7 cells cotransfected with the pNF- κ B-Luc reporter plasmid and Renilla luciferase control reporter vector (pRL-CMV) were treated with the indicated concentrations of OSU-A9 with or without 0.1 nM TNF- α . Luciferase activity as an indicator of NF- κ B-dependent transcription was determined as described in Materials and Methods. Columns, mean; bars, standard deviation ($n = 3$). (C) Western blot analysis of the dose-dependent effects of OSU-A9 on the expression of CXCR4 and Her2 in SKBR3 cells after 48 h exposure in 5% FBS-supplemented Dulbecco's modified Eagle's medium/F-12 medium.

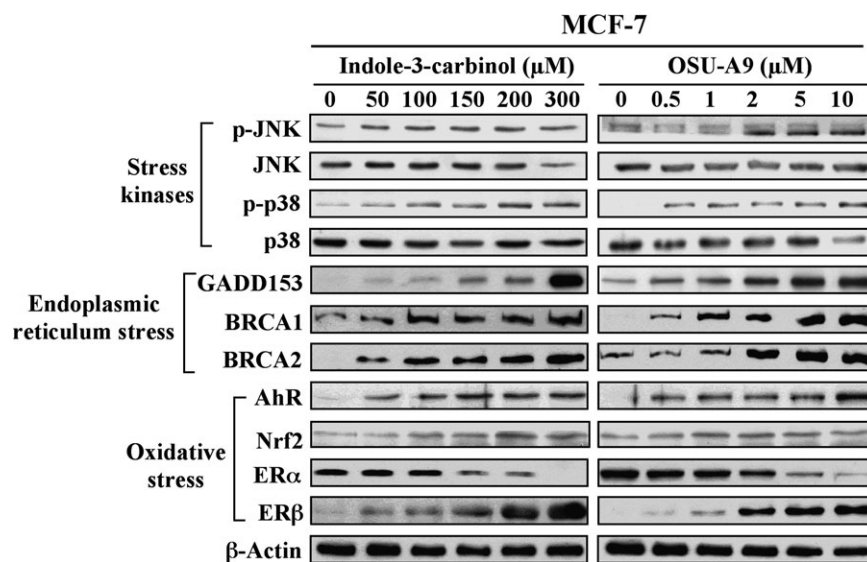


Fig. 3. Activation of stress response signaling by OSU-A9 and indole-3-carbinol. MCF-7 cells were exposed to the indicated concentrations of OSU-A9 and indole-3-carbinol in 5% FBS-supplemented Dulbecco's modified Eagle's medium/F-12 medium for 48 h. Cell lysates were immunoblotted with antibodies against various biomarkers of oxidative stress or endoplasmic reticulum stress, including p-JNK, p-p38, GADD153, BRCA1, BRCA2, AhR, Nrf2, ER α and ER β .

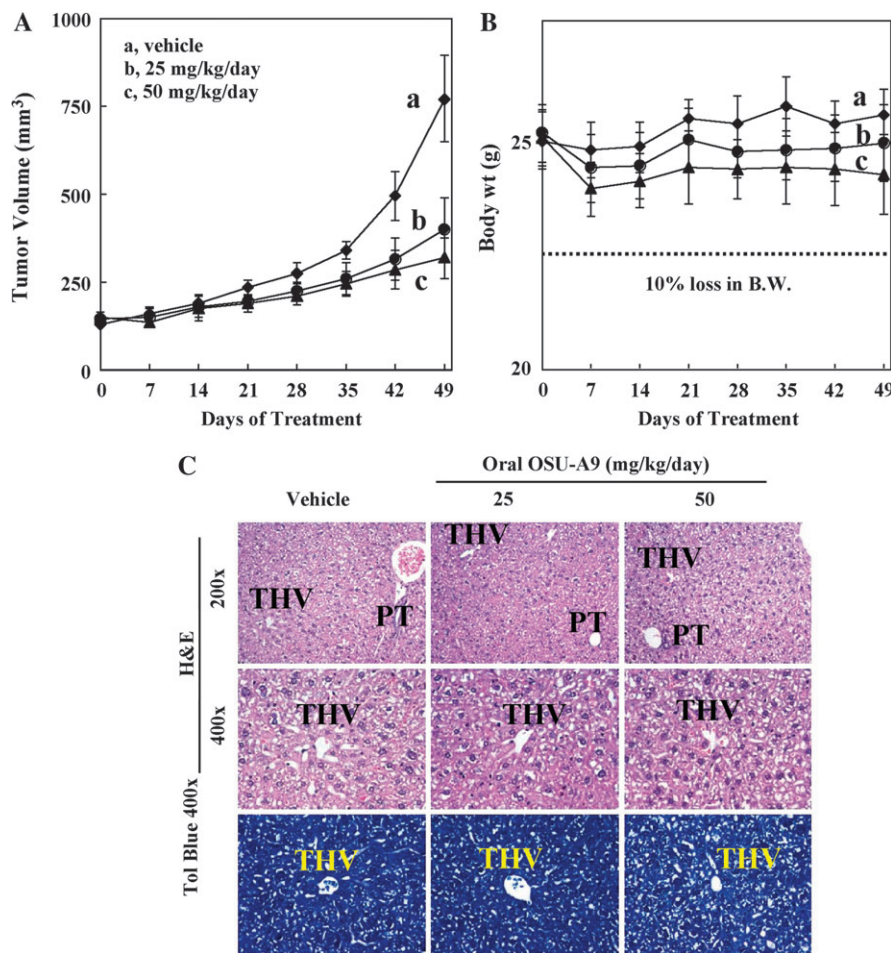


Fig. 4. *In vivo* efficacy of oral OSU-A9. (A) Effect of oral OSU-A9 at 25 and 50 mg/kg/day on the growth of established MCF-7 xenograft tumors in nude mice. Both treatments levels (curves b and c) significantly suppressed tumor growth relative to vehicle-treated controls ($P < 0.01$). Points, mean; bars, standard deviation ($n = 7$). (B) Effect of OSU-A9 at 25 mg/kg/day (curve b) and 50 mg/kg/day (curve c) versus vehicle control (curve a) on body weights of treated animals. Points, mean; bars, standard deviation ($n = 7$). The dashed line represents a calculated 10% loss of body weight. (C) Photomicrographs of representative hematoxylin and eosin- and toluidine blue-stained sections of livers from mice treated as described above. THV, terminal hepatic venule; PT, portal triad; Tol Blue, toluidine blue.

transcription in a NF- κ B-luciferase reporter gene assay (Figure 2B). This inhibition was also manifested by changes in the expression levels of a series of NF- κ B-regulated gene products in MCF-7 cells, including the downregulation of the antiapoptotic proteins survivin, Bcl-2, Bcl-xL and Mcl-1 and the upregulation of the proapoptotic protein Bax (Figure 2A).

We also examined the effect of OSU-A9 on the expression of the chemokine receptor CXCR4, which has been reported to be upregulated by NF- κ B to promote breast cancer metastasis (21–23). Recent evidence indicates that CXCR4 is an essential downstream effector for Her2-mediated breast cancer metastasis to lungs in mice (24) and that silencing of CXCR4 blocked breast cancer metastasis (25). Since MCF-7 cells exhibit a low abundance of endogenous CXCR4 (26), we assessed the effect of OSU-A9 and indole-3-carbinol on the expression of CXCR4 in SKBR3 cells (ER α - β -, Her2+ and CXCR4+). Relative to indole-3-carbinol, OSU-A9 exhibited two orders of magnitude higher potency in ablating CXCR4 expression (Figure 2C). Moreover, this effect was paralleled by a reduction in the expression level of the oncoprotein Her2, which is of high therapeutic relevance considering Her2 overexpression, which occurs in $\sim 30\%$ of breast tumors, is associated with poor clinical outcomes (27).

Stress response signaling

In addition to modulating the Akt–NF- κ B axis, OSU-A9 and indole-3-carbinol activated p38 and JNK in MCF-7 cells (Figure 3), suggest-

ing the involvement of cellular stress responses in the antitumor effects of these agents. These two stress-activated protein kinases are key mediators of apoptosis signaling in response to diverse stimuli associated with the induction of endoplasmic reticulum or oxidative stress, including ultraviolet, γ -irradiation, inflammatory cytokines and chemotherapeutic agents (28,29). The induction of the stress response in OSU-A9- and indole-3-carbinol-treated MCF-7 cells was also borne out by the increased expression of growth arrest- and DNA damage-inducible gene (GADD)153 (also known as CHOP) (Figure 3), a well-recognized endoplasmic reticulum stress-inducible transcription factor (30). GADD153 is involved in apoptosis induction through several distinct mechanisms, including downregulation of Bcl-2 expression and stimulation of reactive oxygen species production (31). Reminiscent of the effects reported previously for indole-3-carbinol and other phytochemicals (32), endoplasmic reticulum stress might underlie the enhanced expression of breast cancer susceptibility gene (BRCA)1 and BRCA2 observed in drug-treated MCF-7 cells, both of which have been identified as tumor suppressors for hormone-responsive cancers (33,34). Evidence indicates that BRCA1 plays a pivotal role in maintaining cell cycle progression and genomic stability (35) and represses the transcriptional activity of ER α through physical interactions (36).

Changes characteristic of cellular response to oxidative stress were also detected in drug-treated MCF-7 cells, including the upregulated expression of AhR and its downstream effector Nrf2 (Figure 3). These

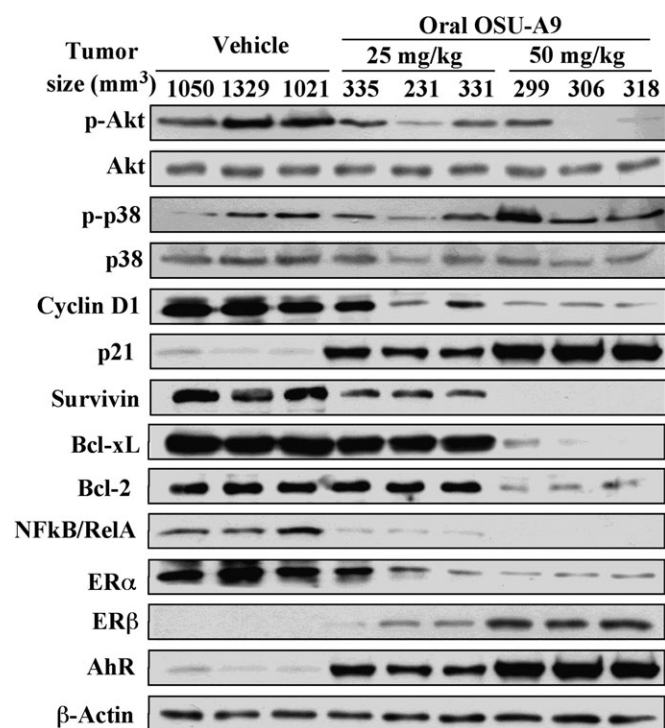


Fig. 5. Western blot analysis of intratumoral biomarkers of drug activity in the homogenates of three representative MCF-7 tumors from each treatment group and their respective final volumes. Tumors were harvested at terminal killing after 49 days of treatment.

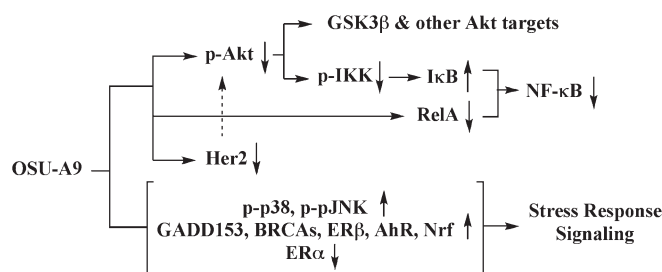


Fig. 6. Diagram depicting the inhibitory and activating effects of OSU-A9 on the Akt–NF-κB signaling axis and stress response signaling, respectively. The ability of OSU-A9 to affect these two signaling networks and thus target different facets of breast malignancy underlies its high potency in suppressing tumor growth.

two transcription factors control the expression of genes encoding antioxidants and xenobiotic detoxification enzymes, such as glutathione-S-transferases and NAD(P)H: quinone oxidase 1, through binding to antioxidant response elements found in their promoters (37). The cross talk between AhR and Nrf2 confers cytoprotection against oxidative stress in non-malignant cells (37,38), which might contribute to the chemopreventive effect of indole-3-carbinol and its metabolite 3,3'-diindolylmethane (5,39). Moreover, oxidative stress has been shown to differentially regulate the expression levels of ER α and ER β in MCF-7 cells (40), which is in line with our finding that OSU-A9 and indole-3-carbinol increased the ratio of the expression levels of ER β to ER α (Figure 3). As ER β antagonizes the function of ER α in promoting estrogen-dependent mammary tumor growth (41), the ability of OSU-A9 to increase the ER β /ER α expression ratio represents potential therapeutic value for the treatment of ER α (+) breast tumors.

Oral OSU-A9 suppresses MCF-7 tumor xenograft growth *in vivo*

To evaluate the *in vivo* antitumor efficacy of OSU-A9, athymic nude mice bearing established subcutaneous MCF-7 tumor xenografts

(mean tumor volume, $145 \pm 14 \text{ mm}^3$) were treated orally by gavage for 49 days with OSU-A9 at 25 or 50 mg/kg daily or with vehicle. As shown in Figure 4A, treatment of mice with 25 and 50 mg/kg daily significantly inhibited MCF-7 tumor growth by 59 and 70%, respectively, relative to vehicle-treated controls ($P < 0.01$). Importantly, all mice appeared to tolerate the daily oral administration of OSU-A9 without overt signs of toxicity, as indicated by a lack of significant loss in body weight (Figure 4B; the dashed line indicates a hypothetical 10% loss in body weight), the absence of gross lesions at necropsy and normal hematological and serum chemistry parameters (data not shown).

Centrilobular hepatocellular hypertrophy is a morphologic marker of sustained enzyme induction in the rodent (42), and changes in toluidine blue staining can be used to discriminate the proliferation of smooth endoplasmic reticulum that occurs in association with enzyme induction (43). Accordingly, formalin-fixed, paraffin-embedded liver sections from these OSU-A9-treated mice were stained with hematoxylin and eosin or toluidine blue and evaluated microscopically. As shown in Figure 4C, no lesions were evident in hematoxylin and eosin-stained livers of drug-treated mice. Livers from all experiment groups exhibited a uniform size of hepatocytes across the hepatic lobule. Similarly, no apparent differences were observed in toluidine blue staining among experimental groups. These results suggest that OSU-A9 administered orally as described here is not a significant inducer of the biotransformation enzymatic system.

To correlate the *in vivo* tumor-suppressive response to mechanisms identified *in vitro*, the effects of OSU-A9 on 11 representative intratumoral biomarkers of drug activity were evaluated by immunoblotting of MCF-7 tumor homogenates collected after 49 days of treatment. These biomarkers included the phosphorylation status of Akt and p38 and expression levels of cyclin D1, p21, survivin, Bcl-xL, Bcl-2, NF-κB/RelA, ER α , ER β and AhR. As shown in Figure 5, the effects of OSU-A9 on these biomarkers were qualitatively similar to those observed *in vitro* and reflect the dose-dependent tumor suppression *in vivo*. Treatment with oral OSU-A9 at 25 and 50 mg/kg/day induced marked, dose-dependent reductions in intratumoral levels of p-Akt, cyclin D1, survivin, Bcl-xL, Bcl-2, RelA and ER α accompanied by increases in intratumoral levels of p-p38, p21, ER β and AhR. Together, these findings indicate the oral bioavailability of OSU-A9 and an *in vivo* antitumor activity that is mediated through the modulation of Akt–NF-κB and stress response pathways.

Discussion

We demonstrate here that OSU-A9, a structurally optimized derivative of indole-3-carbinol, is a potent antitumor agent with a unique ability to target a broad spectrum of signaling pathways, which, based on our findings, can be categorized into two functional lineages: the Akt–NF-κB axis and stress response signaling (Figure 6). While broader effects that encompass other targets and pathways cannot be ruled out, our data show that modulation of Akt–NF-κB and stress response signaling pathways by OSU-A9 is important for its antitumor activity against breast cancer cells. The ability of OSU-A9 to interfere with the interplay between these two signaling networks suggests its therapeutic potential for the treatment of endocrine-resistant and/or highly metastatic breast cancers. For example, in addition to Akt signaling, NF-κB controls the ability of malignant cells to resist apoptosis-based tumor surveillance mechanisms (44), which endows endocrine or chemotherapeutic resistance to ER(+) breast cancer cells (45). Moreover, as the cross talk between Her2 and CXCR4 promotes breast tumor metastasis (24), the concerted suppressive effect of OSU-A9 on the expression of these oncogenic proteins represents a novel strategy to block HER2-mediated invasion.

In addition, the ability of OSU-A9 to increase the expression ratio of ER β to ER α , as well as the expression of BRCA1 and BRCA2 is

noteworthy. The ratio of ER β /ER α expression in breast tumors is lower than in normal breast tissues due to a lower expression of ER β . It has been reported that ER β reduced ER α activation-induced cell proliferation by antagonizing ER α signaling (46,47) and that decreased ER β expression characterizes the malignant progression of breast cancer (48). Thus, this increased ER β :ER α ratio, in conjunction with BRCA1-mediated repression of ER α -dependent gene expression, suggests the possibility that OSU-A9 could improve the clinical outcome of ER(+) patients.

Furthermore, the ability of OSU-A9 to upregulate the expression of AhR and its downstream target Nrf2 underscores its potential translational value in breast cancer prevention. These two transcription factors activate the expression of a series of cytoprotective enzymes involved in carcinogen detoxification, thereby protecting cells against carcinogen-induced tumorigenesis (37,39).

Despite this complicated mode of action, non-malignant MCF-10A mammary epithelial cells were resistant to OSU-A9's antiproliferative effects, consistent with the observed tolerance of nude mice to this drug. Daily oral administration of OSU-A9 at 50 mg/kg for 49 days in MCF-7 tumor-bearing nude mice did not give rise to overt signs of toxicity. Moreover, indole-3-carbinol, OSU-A9's parent compound, was reported to cause centrilobular hepatocellular hypertrophy and to induce hepatic Phase I and Phase II enzymes in rodents (7,49,50), findings which underlie the controversy over the role of dietary indole-3-carbinol in increased incidences of uterine adenocarcinoma in animal models (49). The possibility that the enhanced apoptotic activity of OSU-A9 could be associated with an increased ability to induce these hepatic changes was refuted by the finding that OSU-A9 did not cause changes in indicators of hepatotoxicity or cytochrome P450 enzyme induction. Based on these data, OSU-A9 is not a significant inducer of the biotransformation enzymatic system.

In conclusion, the results of this investigation suggest the translational value of OSU-A9 in the treatment or prevention of breast cancer. Not only does OSU-A9 retain the ability of indole-3-carbinol to target different facets of oncogenic signaling in breast cancer cells but also does so with 100-fold higher potency and without the hepatic changes associated with indole-3-carbinol exposure. Testing of the efficacy of OSU-A9 in other breast cancer models of clinical relevance is currently underway.

Funding

National Cancer Institute (R01CA112250 and R21CA135560) to C.-S.C.; National Science Council (Taiwan) (NSC 96-2320-B-039-021-MY3) to J.-R.W.

Acknowledgements

The authors would like to thank Dr Robert Brueggemeier (The Ohio State University) and Dr Cheng-Wen Lin (China Medical University, Taichung, Taiwan) for the kind gifts of MCF-10A cells and the pNF- κ B-Luc reporter plasmid, respectively.

Conflict of Interest Statement: None declared.

References

- Frantz,S. (2005) Drug discovery: playing dirty. *Nature*, **437**, 942–943.
- Reed,G.A. *et al.* (2005) A phase I study of indole-3-carbinol in women: tolerability and effects. *Cancer Epidemiol. Biomarkers Prev.*, **14**, 1953–1960.
- Reed,G.A. *et al.* (2006) Single-dose and multiple-dose administration of indole-3-carbinol to women: pharmacokinetics based on 3,3'-diindolylmethane. *Cancer Epidemiol. Biomarkers Prev.*, **15**, 2477–2481.
- Aggarwal,B.B. *et al.* (2005) Molecular targets and anticancer potential of indole-3-carbinol and its derivatives. *Cell Cycle*, **4**, 1201–1215.
- Kim,Y.S. *et al.* (2005) Targets for indole-3-carbinol in cancer prevention. *J. Nutr. Biochem.*, **16**, 65–73.
- Manson,M.M. (2005) Inhibition of survival signalling by dietary polyphenols and indole-3-carbinol. *Eur. J. Cancer*, **41**, 1842–1853.
- Rogan,E.G. (2006) The natural chemopreventive compound indole-3-carbinol: state of the science. *In Vivo*, **20**, 221–228.
- Weng,J.R. *et al.* (2008) Indole-3-carbinol as a chemopreventive and anticancer agent. *Cancer Lett.*, **262**, 153–163.
- Auborn,K.J. *et al.* (2003) Indole-3-carbinol is a negative regulator of estrogen. *J. Nutr.*, **133**, 2470S–2475S.
- Wang,T.T. *et al.* (2006) Estrogen receptor alpha as a target for indole-3-carbinol. *J. Nutr. Biochem.*, **17**, 659–664.
- Parkin,D.R. *et al.* (2004) Differences in the hepatic P450-dependent metabolism of estrogen and tamoxifen in response to treatment of rats with 3,3'-diindolylmethane and its parent compound indole-3-carbinol. *Cancer Detect. Prev.*, **28**, 72–79.
- Chao,W.R. *et al.* (2007) Computer-aided rational drug design: a novel agent (SR13668) designed to mimic the unique anticancer mechanisms of dietary indole-3-carbinol to block Akt signaling. *J. Med. Chem.*, **50**, 3412–3415.
- Kassouf,W. *et al.* (2006) Inhibition of bladder tumor growth by 1,1-bis(3'-indolyl)-1-(p-substitutedphenyl)methanes: a new class of peroxisome proliferator-activated receptor gamma agonists. *Cancer Res.*, **66**, 412–418.
- Cho,S.D. *et al.* (2007) Nur77 agonists induce proapoptotic genes and responses in colon cancer cells through nuclear receptor-dependent and nuclear receptor-independent pathways. *Cancer Res.*, **67**, 674–683.
- Brandi,G. *et al.* (2003) A new indole-3-carbinol tetrameric derivative inhibits cyclin-dependent kinase 6 expression, and induces G1 cell cycle arrest in both estrogen-dependent and estrogen-independent breast cancer cell lines. *Cancer Res.*, **63**, 4028–4036.
- Weng,J.R. *et al.* (2007) A potent indole-3-carbinol derived antitumor agent with pleiotropic effects on multiple signaling pathways in prostate cancer cells. *Cancer Res.*, **67**, 7815–7824.
- Chinni,S.R. *et al.* (2002) Akt inactivation is a key event in indole-3-carbinol-induced apoptosis in PC-3 cells. *Clin. Cancer Res.*, **8**, 1228–1236.
- Rahman,K.M. *et al.* (2004) Inactivation of akt and NF-kappaB play important roles during indole-3-carbinol-induced apoptosis in breast cancer cells. *Nutr. Cancer*, **48**, 84–94.
- Mitsuuchi,Y. *et al.* (2000) The phosphatidylinositol 3-kinase/AKT signal transduction pathway plays a critical role in the expression of p21WAF1/CIP1/SDI1 induced by cisplatin and paclitaxel. *Cancer Res.*, **60**, 5390–5394.
- Sa,G. *et al.* (2004) P27 expression is regulated by separate signaling pathways, downstream of Ras, in each cell cycle phase. *Exp. Cell Res.*, **300**, 427–439.
- Helbig,G. *et al.* (2003) NF-kappaB promotes breast cancer cell migration and metastasis by inducing the expression of the chemokine receptor CXCR4. *J. Biol. Chem.*, **278**, 21631–21638.
- Kukreja,P. *et al.* (2005) Up-regulation of CXCR4 expression in PC-3 cells by stromal-derived factor-1alpha (CXCL12) increases endothelial adhesion and transendothelial migration: role of MEK/ERK signaling pathway-dependent NF-kappaB activation. *Cancer Res.*, **65**, 9891–9898.
- Rahman,K.M. *et al.* (2006) Therapeutic intervention of experimental breast cancer bone metastasis by indole-3-carbinol in SCID-human mouse model. *Mol. Cancer Ther.*, **5**, 2747–2756.
- Li,Y.M. *et al.* (2004) Upregulation of CXCR4 is essential for HER2-mediated tumor metastasis. *Cancer Cell*, **6**, 459–469.
- Liang,Z. *et al.* (2005) Silencing of CXCR4 blocks breast cancer metastasis. *Cancer Res.*, **65**, 967–971.
- Ueda,Y. *et al.* (2006) Deletion of the COOH-terminal domain of CXC chemokine receptor 4 leads to the down-regulation of cell-to-cell contact, enhanced motility and proliferation in breast carcinoma cells. *Cancer Res.*, **66**, 5665–5675.
- Slamon,D.J. *et al.* (1989) Studies of the HER-2/neu proto-oncogene in human breast and ovarian cancer. *Science*, **244**, 707–712.
- Zarubin,T. *et al.* (2005) Activation and signaling of the p38 MAP kinase pathway. *Cell Res.*, **15**, 11–18.
- Liu,J. *et al.* (2005) Role of JNK activation in apoptosis: a double-edged sword. *Cell Res.*, **15**, 36–42.
- Oyadomari,S. *et al.* (2004) Roles of CHOP/GADD153 in endoplasmic reticulum stress. *Cell Death Differ.*, **11**, 381–389.
- McCullough,K.D. *et al.* (2001) Gadd153 sensitizes cells to endoplasmic reticulum stress by down-regulating Bcl2 and perturbing the cellular redox state. *Mol. Cell. Biol.*, **21**, 1249–1259.
- Fan,S. *et al.* (2006) BRCA1 and BRCA2 as molecular targets for phytochemicals indole-3-carbinol and genistein in breast and prostate cancer cells. *Br. J. Cancer*, **94**, 407–426.
- Struwing,J.P. *et al.* (1997) The risk of cancer associated with specific mutations of BRCA1 and BRCA2 among Ashkenazi Jews. *N. Engl. J. Med.*, **336**, 1401–1408.

34. Thompson, D. *et al.* (2002) Cancer incidence in BRCA1 mutation carriers. *J. Natl Cancer Inst.*, **94**, 1358–1365.
35. Deng, C.X. (2006) BRCA1: cell cycle checkpoint, genetic instability, DNA damage response and cancer evolution. *Nucleic Acids Res.*, **34**, 1416–1426.
36. Wang, C. *et al.* (2005) Cyclin D1 antagonizes BRCA1 repression of estrogen receptor alpha activity. *Cancer Res.*, **65**, 6557–6567.
37. Kohle, C. *et al.* (2007) Coordinate regulation of Phase I and II xenobiotic metabolisms by the Ah receptor and Nrf2. *Biochem. Pharmacol.*, **73**, 1853–1862.
38. Miao, W. *et al.* (2005) Transcriptional regulation of NF-E2 p45-related factor (NRF2) expression by the aryl hydrocarbon receptor-xenobiotic response element signaling pathway: direct cross-talk between phase I and II drug-metabolizing enzymes. *J. Biol. Chem.*, **280**, 20340–20348.
39. Kohle, C. *et al.* (2006) Activation of coupled Ah receptor and Nrf2 gene batteries by dietary phytochemicals in relation to chemoprevention. *Biochem. Pharmacol.*, **72**, 795–805.
40. Tamir, S. *et al.* (2002) The effect of oxidative stress on ERalpha and ERbeta expression. *J. Steroid Biochem. Mol. Biol.*, **81**, 327–332.
41. Hayashi, S.I. *et al.* (2003) The expression and function of estrogen receptor alpha and beta in human breast cancer and its clinical application. *Endocr. Relat. Cancer*, **10**, 193–202.
42. Grasso, P. *et al.* (1991) Role of persistent, non-genotoxic tissue damage in rodent cancer and relevance to humans. *Annu. Rev. Pharmacol. Toxicol.*, **31**, 253–287.
43. Sargeant, A.M. *et al.* (2007) Chemopreventive and bioenergetic signaling effects of PDK1/Akt pathway inhibition in a transgenic mouse model of prostate cancer. *Toxicol. Pathol.*, **35**, 549–561.
44. Karin, M. (2006) NF-kappaB and cancer: mechanisms and targets. *Mol. Carcinog.*, **45**, 355–361.
45. Zhou, Y. *et al.* (2005) The NFkappaB pathway and endocrine-resistant breast cancer. *Endocr. Relat. Cancer*, **12** (suppl. 1): S37–S46.
46. Lazennec, G. *et al.* (2001) ER beta inhibits proliferation and invasion of breast cancer cells. *Endocrinology*, **142**, 4120–4130.
47. Sotoca, A.M. *et al.* (2008) Influence of cellular ERalpha/ERbeta ratio on the ERalpha-agonist induced proliferation of human T47D breast cancer cells. *Toxicol. Sci.*, **105**, 303–311.
48. Shaaban, A.M. *et al.* (2003) Declining estrogen receptor-beta expression defines malignant progression of human breast neoplasia. *Am. J. Surg. Pathol.*, **27**, 1502–1512.
49. Yoshida, M. *et al.* (2004) Dietary indole-3-carbinol promotes endometrial adenocarcinoma development in rats initiated with N-ethyl-N'-nitro-N-nitrosoguanidine, with induction of cytochrome P450s in the liver and consequent modulation of estrogen metabolism. *Carcinogenesis*, **25**, 2257–2264.
50. Crowell, J.A. *et al.* (2006) Indole-3-carbinol, but not its major digestive product 3,3'-diindolylmethane, induces reversible hepatocyte hypertrophy and cytochromes P450. *Toxicol. Appl. Pharmacol.*, **211**, 115–123.

Received April 7, 2009; revised July 7, 2009; accepted August 1, 2009